

Expanded View Figures

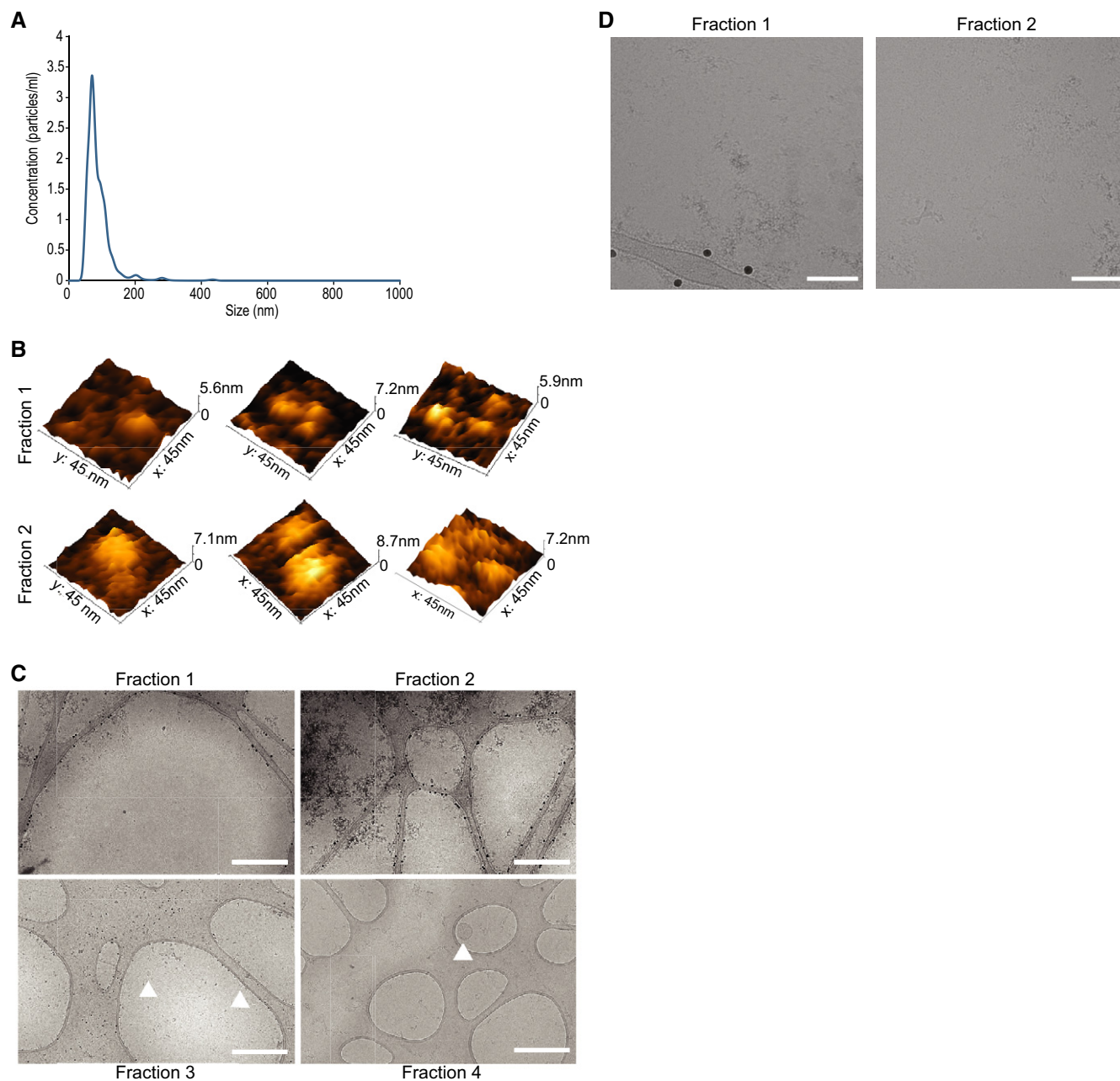


Figure EV1. AF4 analysis separation of *Pf*-derived EVs.

- A Nanotrack particle analysis (NTA) of the input *Pf*-derived EVs. Assessment of total *Pf*-derived EVs using NanoSight® particle analyzer detecting particles in a diameter mode of 70 nm. The concentration is approximately 10^{12} particles/ml. This experiment is representative of three biological replicates.
- B Representative 3D AFM images of particles from fractions 1 and 2.
- C Representative cryo-TEM images at low magnification of fractions 1–4 to illustrate sample purity and isolation of extracellular proteins (fractions 1 and 2) from extracellular vesicles (fractions 3 and 4). Scale bar—500 nm. Arrowheads indicate EVs.
- D Cryo-TEM images of fractions 1 and 2 highlighting bio-molecular aggregates. Scale bar—100 nm.

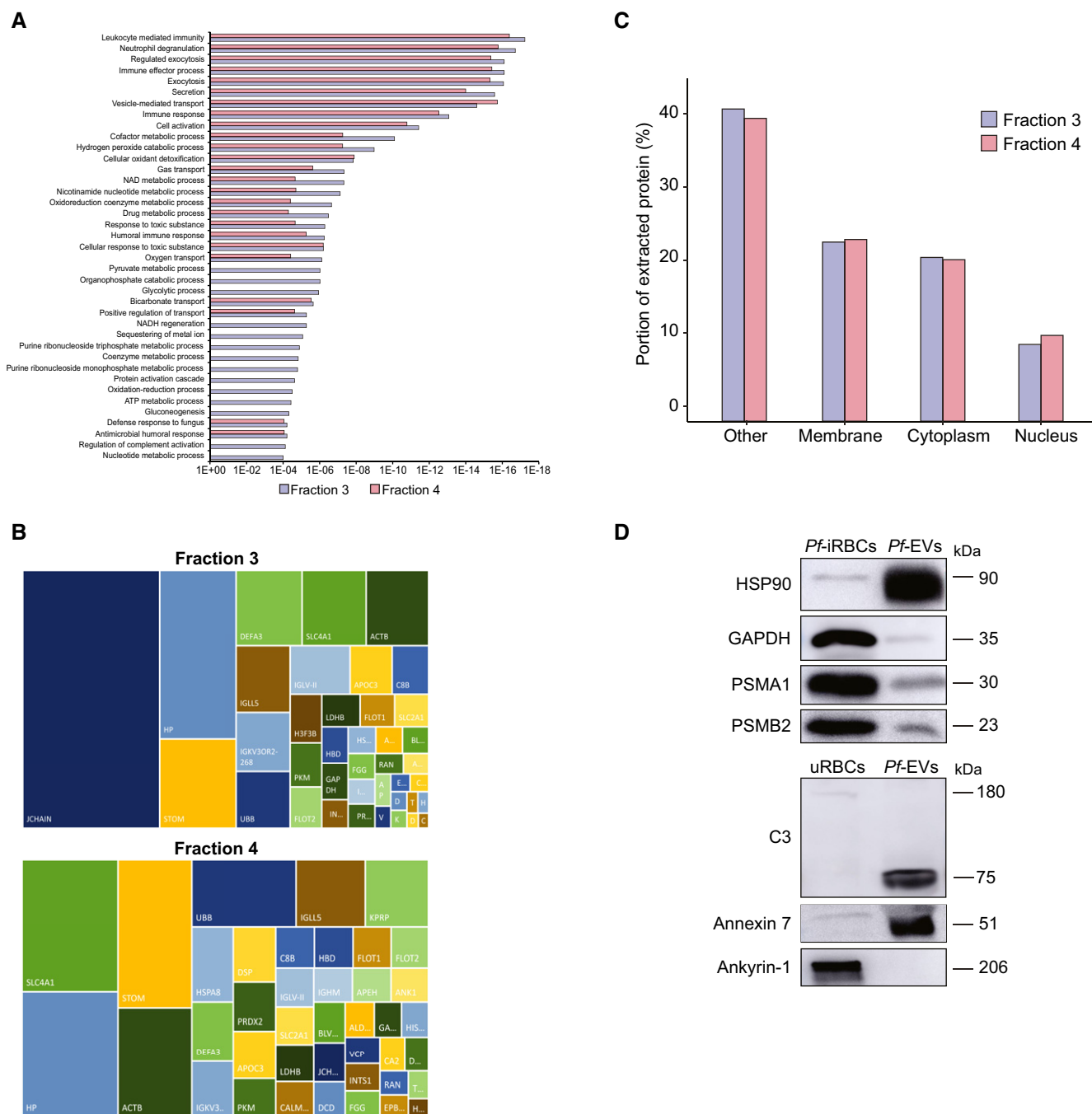


Figure EV2. Proteomic analysis of *Pf*-derived EV subpopulations.

Total proteins were extracted from the two EV fractions (F3 and F4) and subjected to LC-MS/MS analysis.

A GO annotation analysis of the two EV fractions.

B The figure presents the most intense proteins in the EV repertoire (not including the HBB and HBA dominant proteins). The rectangular areas are proportional to the median intensity of the protein in either F3 or F4 EVs.

C Subcellular localization of identified proteins by GO annotation. Other—mitochondria, early and late endosome, lysosome, cytoskeleton, secreted, and so on. Quantification and averaging of four independent biological replicates. Reference list: *Homo sapiens* or *Plasmodium falciparum* (all genes in the database).

D Western blot analysis of uRBCs or iRBCs and *Pf*-derived EVs. Anti-PSMA1, anti-PSMB2 (proteasome subunits) and anti-C3 (complement system protein) antibodies were used. As a positive control, antibodies against the EV markers HSP90 and Annexin 7 were used. C3b subunit is detected within *Pf*-derived EVs. As a negative control, antibodies against the RBC membrane marker Ankyrin-1 were used.

Source data are available online for this figure.

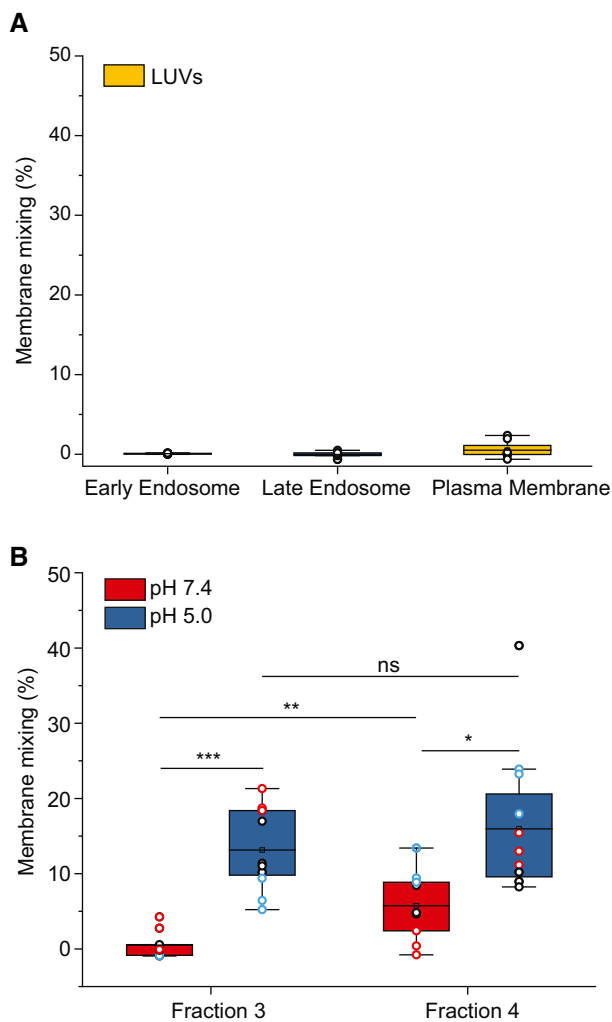


Figure EV3. FRET assay controls.

A FRET-based membrane mixing for LUVs–LUVs interaction (negative control) under the three tested conditions (plasma membrane, early endosome and late endosomes). No significant fusion is observed. Each dot represents one data point, with the whole dataset obtained from $n = 3$ biological repeats (colored symbols) with three technical repeats each. Box layouts represent 25–75% of the distribution, whiskers highlight outlier data points, and horizontal black lines represent the mean of the distribution.

B Comparison of membrane mixing between F3-EVs and F4-EVs at late endosomal conditions (pH 5.0, blue) and interaction with the same liposomes at neutral pH (red). Significant membrane mixing is observed post acidification for F3-EVs ($P = 0.0009$) and F4-EVs ($P = 0.017$). A significant difference in membrane mixing between the two fractions is observed at pH 7.4 ($P = 0.006$). No significant difference in membrane mixing between the two fractions is observed at pH 5 ($P = 0.375$). Three independent experiments were performed and a two-sample t-test was applied. Each dot represents one data point, with the whole dataset obtained from $n = 3$ biological repeats (colored symbols) with three technical repeats each. Box layouts represent 25–75 percentiles of the distribution, whiskers highlight outlier data points and horizontal black lines represent the mean of the distribution. * $P \leq 0.05$, ** $P \leq 0.01$, *** $P < 0.001$.

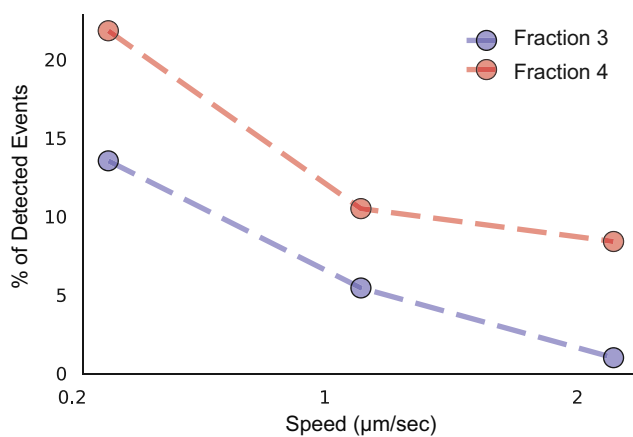
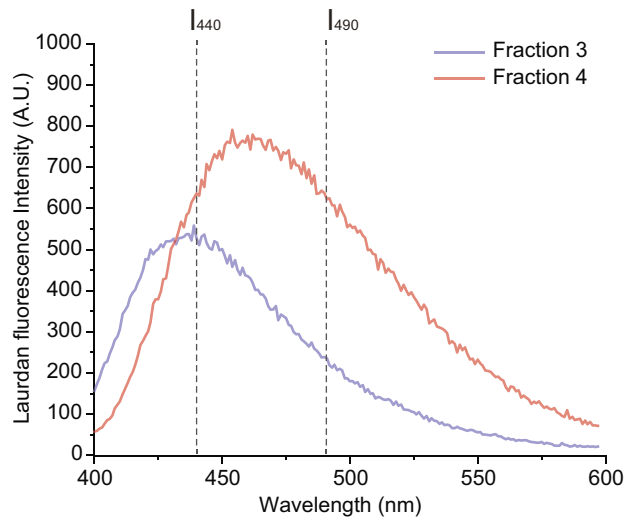
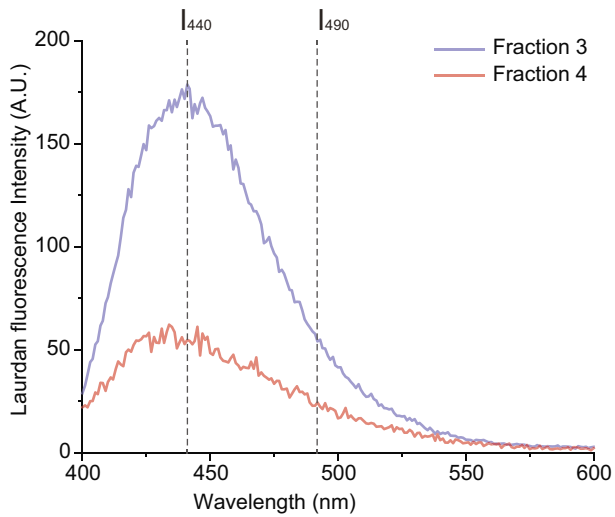


Figure EV4. Laurdan spectra for additional biological repeats.

Characteristic Laurdan spectra for F3-EVs and F4-EVs for the second and third biological repeat, as shown in Fig 6, display a predominant peak at 440 nm for F3-EVs, indicating a high lipid packing, and a shift towards 490 nm emission for F4-EVs.

Figure EV5. Percentage of detected events as a function of the AFM tip approach speed for fractions 3 and 4.